The Eighth International
Symposium of Robotics Research
Hayama, Japan, October 3-7, 1997

Elastic Strips: Real-Time Path Modification for Mobile Manipulation

Oliver Brock Oussama Khatib
Robotics Laboratory, Department of Computer Science
Stanford University, Stanford, California 94305
email: {oli | khatib}@CS.Stanford.EDU

Abstract

The elastic strip framework presented in this paper is a new approach to real-time obstacle avoidance for robots with many degrees of freedom. The avoidance behavior can be integrated with task execution, a capability necessary for the application of mobile manipulation to dynamic real-world environments. The elastic strip initially represents a collision-free path generated by a planner. As the environment changes, the elastic strip is incrementally modified to maintain a smooth, collision-free path. Since the elastic strip is entirely represented in workspace, costly computation in a high-dimensional configuration space is avoided. This results in an efficient modification procedure for the elastic strip, even for robots with many degrees of freedom. The general framework of elastic strips is introduced and its application to obstacle avoidance during task execution is discussed.

1 Introduction

The robust execution of planned robot motion in dynamic environments and in the presence of uncertainty is essential for achieving intelligent robot behavior. In mobile manipulation this problem becomes particularly challenging because the execution of a task has to be integrated with reactive collision avoidance for robots with many degrees of freedom.

Recent research in control structures for mobile manipulation has resulted in an effective approach to task description and execution for arm/base systems at the object level (Khatib et al. 1996). Compliant motion and force control strategies allow multiple arm/base systems to cooperate with a decentralized control structure, accomplishing complex manipulation tasks.

Reactive collision avoidance for manipulators or mobile platforms is a well-studied problem (Krogh 1984; Khatib 1986; Arkin 1987; Latombe 1991). Due to the recent interest in mobile manipulation more advanced methods are being investigated to incorporate obstacle avoidance with limited coordination between manipulator and mobile base (Carriker et al. 1989; Seraji 1993; Yamamoto and Yun 1995; Nassal 1996). These approaches are mainly concerned with positioning the base according to a manipulator-dependent cost function and suspend task-level behavior to perform collision avoidance. Mobile manipulation, however, requires obstacle avoidance during task execution.

In this paper we present a new approach to real-time path modification for robotic systems with many degrees of freedom. It extends the elastic band framework proposed in Quinlan and Khatib 1993. The new approach, called the *elastic strip*, is an efficient framework for collision avoidance for robots with many degrees of freedom. In addition, it allows for the integration of collision avoidance with the execution of manipulation tasks. Furthermore, it maintains the topological properties of the path and therefore is immune to local minima.

The efficiency of this approach is based on the fact that all computations are carried out directly in the workspace, avoiding the computational complexity of high-dimensional configuration spaces. We present the general algorithm and illustrate coordination schemes for obstacle avoidance and task execution.

2 Arm/Base Coordination

The operational space equations of motion of a manipulator are (Khatib 1987)

$$\Lambda(\mathbf{x})\ddot{\mathbf{x}} + \mu(\mathbf{x}, \dot{\mathbf{x}}) + \mathbf{p}(\mathbf{x}) = \mathbf{F}, \qquad (1)$$

where $\mathbf{x}$ is the vector of the m operational coordinates describing the position and orientation of the effector, and $\Lambda(\mathbf{x})$ is the $m \times m$ kinetic energy matrix associated with the operational space. $\mu(\mathbf{x}, \dot{\mathbf{x}})$, $\mathbf{p}(\mathbf{x})$, and $\mathbf{F}$ are respectively the centrifugal and Coriolis force vector, gravity force vector, and generalized force vector acting in operational space.

These equations of motion describe the dynamic response of a manipulator to the application of an operational force $\mathbf{F}$ at the end effector. For non-redundant manipulators, the relationship between operational forces $\mathbf{F}$ and joint forces $\mathbf{\Gamma}$ is

$$\mathbf{\Gamma} = J^T(\mathbf{q})\mathbf{F}, \tag{2}$$

where $J(\mathbf{q})$ is the Jacobian matrix.

For redundant systems it can be shown that the relationship between joint torques and operational forces is

$$\mathbf{\Gamma} = J^T(\mathbf{q})\mathbf{F} + \left[I - J^T(\mathbf{q})\overline{J}^T(\mathbf{q})\right]\mathbf{\Gamma}_0, \tag{3}$$

with

$$\overline{J}(\mathbf{q}) = A^{-1}(\mathbf{q})J^T(\mathbf{q})\Lambda(\mathbf{q}), \tag{4}$$

where $\overline{J}(\mathbf{q})$ is the dynamically consistent generalized inverse. This relationship provides a decomposition of joint forces into two dynamically decoupled control vectors: joint forces corresponding to forces acting at the end effector ($J^T\mathbf{F}$) and joint forces that only affect internal motions, $\left([I - J^T(\mathbf{q})\overline{J}^T(\mathbf{q})]\mathbf{\Gamma}_0\right)$.

Using this decomposition, the end effector can be controlled by operational forces, whereas internal motions can be independently controlled by joint forces that are guaranteed not to alter the end effector's dynamic behavior.

This can be applied to integrate task behavior with task-independent behavior, such as collision avoidance. In equation (3) $\mathbf{F}$ are the commanded forces at the end-effector to accomplish the task and $\mathbf{\Gamma}_0$ are the joint forces mapped into the null space to implement task-independent behavior.

3 Elastic Band Framework

3.1 Overview

An elastic band (Quinlan and Khatib 1993) is a discretized curve in the configuration space of a robot, representing a collision-free path. This path is initially obtained from a motion planner and subsequently subjected to artificial forces. Objects in the environment exert external, repulsive forces on the elastic band, ensuring obstacle avoidance. Internal forces act to shorten and smoothen the path, imitating the physical behavior of elastic material. The framework has been extended to non-holonomic robots (Khatib et al. 1997).

The key ingredient for the efficiency of the modification procedure for the elastic band is the description of local free space around it. With only one distance computation in the workspace a hypersphere of free configuration space can be computed. This hypersphere is called *bubble* (Quinlan 1994). By covering the entire elastic band with overlapping bubbles we can guarantee that the path it represents is collision-free. This is illustrated in Figure 1.

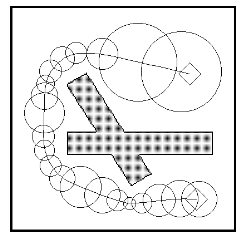

Figure 1: Bubbles on an Elastic Band

3.2 Limitations

The elastic band framework represents the trajectory of the robot and the local free space around it in the configuration space. This entails disadvantages that make an application of the approach to mobile manipulation difficult.

In mobile manipulation the task is described in terms of end-effector motions. A joint space trajectory is an unnatural representation for this motion. Since the elastic band approach is based on joint space trajectories, it is impractical for application to mobile manipulation.

In the elastic band framework the estimate of the local free space around a configuration becomes excessively conservative, as the number of degrees of freedom of the manipulator increases (Quinlan 1994). As a consequence, an excessive amount of bubbles is needed to cover the elastic band, affecting the real-time performance of the algorithm.

4 Elastic Strip Framework

4.1 Overview

The basic idea of the *elastic strip* framework is similar to elastic bands (Quinlan and Khatib 1993). A trajectory is incrementally modified by external forces originating from obstacles in the environment and internal forces are applied to shorten and smoothen it.

To minimize the impact of the dimensionality of the configuration space on the computational complexity of the algorithm and thereby its real-time performance, we choose to represent the trajectory in the workspace.

Whereas with elastic bands a configuration of the robot could be described as a point in configuration space, a workspace description of that configuration consists of the robot's workspace volume. Similarly, in the elastic band framework a bubble represents a configuration free space hypersphere; this corresponds to an obstacle-free workspace volume in the new approach.

A robot trajectory will then be represented by the workspace volume swept by the robot during the motion along the path, as opposed to a one-dimensional curve in configuration space. This volume can be imagined as a strip of elastic material that is deformed by obstacles and shortens when obstacles are removed.

The behavior of the elastic strip differs in certain aspects from elastic material. Since we are not restrained by the physical laws of elasticity, we choose the effect of forces on the elastic strip to be task dependent, thereby integrating collision avoidance and task execution.

4.2 Rigid Body Representation

During the execution of a trajectory a robot sweeps out a volume in the workspace. The trajectory is collision-free if no obstacle is inside this volume. To warrant collision avoidance the volume has to be computed using a model of the rigid bodies in motion and checked against obstacles in the environment.

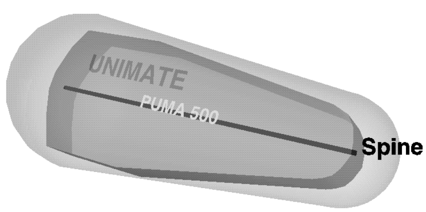

Figure 2: Illustration of a spine

A rigid body can be approximated by a line segment that is parameterized by a varying width. We call that line segment the *spine* of the rigid body. The width specifies the free space required around the line segment for the body to be collision free. In Figure 2 the spine of a transparent PUMA 560 link is shown as the black line along its central axis; the volume associated with the spine encloses the link.

As a rigid body comes closer to obstacles, the model described above might result in incorrect collision detection. To address this difficulty the representation of rigid bodies can be generalized to describe rigid bodies at an arbitrary level of detail.

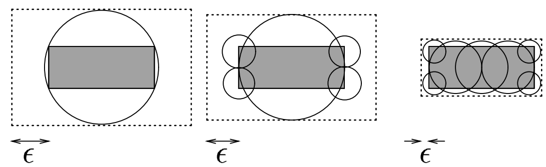

Figure 3: Covering a body with spines

The basic idea of this generalization is to introduce more spines to cover the volume of the rigid body with increasing accuracy as the distance to obstacles decreases. In Figure 3 the rectangular cross section of a body and its circular covering by spines are shown for different resolutions δ_i, indicated by the dotted region. The three pictures could also be interpreted as the evolution of the volume description as the rigid body approaches an obstacle at distance δ_i.

For the sake of simplicity we assume in the remainder of this paper that the volume of a rigid body is described by a single spine.

4.3 Representing Local Free Space

To compute a bubble in the elastic band approach, a distance measurement to a point in the workspace has to be translated into a hypersphere in configuration space. When the free space is represented in the workspace, the distance computation translates directly into a bubble in the workspace. Let $\rho(\mathbf{p})$ be the function that computes the minimum distance from a point $\mathbf{p}$ to any obstacle. The *workspace bubble* of free space around $\mathbf{p}$ is defined as

$$\mathcal{B}(\mathbf{p}) = \{ \mathbf{q} : \|\mathbf{p} - \mathbf{q}\| < \rho(\mathbf{p}) \}.$$

An approximation of the local free space around a rigid body b in configuration q can be computed by generating a set of workspace bubbles centered on the spine. This set of bubbles is called *protective hull* $\mathcal{P}_q^b$. The local free space or protective hull $\mathcal{P}_q^{\mathcal{R}}$ of a robot $\mathcal{R}$ at a configuration q is described by the union of protective hulls of each rigid body of $\mathcal{R}$,

$$\mathcal{P}_q^{\mathcal{R}} = \bigcup_{b \in \mathcal{R}} \mathcal{P}_q^b.$$

Figure 4 shows a protective hull of the *Stanford Mobile Platform*. Note that a single workspace bubble may contain multiple rigid bodies or even the entire robot, implying that for large clearances a simple description of the local free space suffices.

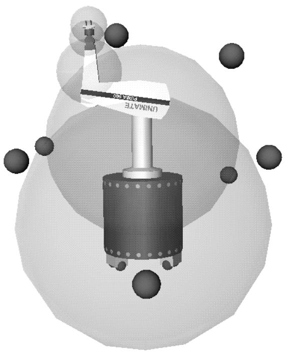

Figure 4: Protective hull of the Stanford Mobile Platform amidst spherical obstacles

4.4 Connectedness of Elastic Strip

An elastic strip $\mathcal{S}_{\mathcal{T}}^{\mathcal{R}} = (\mathcal{P}_1^{\mathcal{R}}, \mathcal{P}_2^{\mathcal{R}}, \mathcal{P}_3^{\mathcal{R}}, \cdots, \mathcal{P}_n^{\mathcal{R}})$ is a sequence of protective hulls $\mathcal{P}_i^{\mathcal{R}}$ representing the local free space of a configuration q_i on the trajectory $\mathcal{T}$ of the robot $\mathcal{R}$.

Since each configuration q_i is guaranteed to be free of collisions by the protective hull $\mathcal{P}_{q_i}^{\mathcal{R}}$, it remains to be shown that the union of all protective hulls contains the volume $V_{\mathcal{T}}^{\mathcal{R}}$ swept by the robot along the trajectory. The condition of feasibility of trajectory $\mathcal{T}$ described by $\mathcal{S}_{\mathcal{T}}^{\mathcal{R}}$ is

$$V_{\mathcal{T}}^{\mathcal{R}} \subseteq V_{\mathcal{S}}^{\mathcal{R}} = \bigcup_{1 \leq i \leq n} \mathcal{P}_i^{\mathcal{R}}. \qquad (5)$$

This illustrated in Figure 5, where three consecutive protective hulls cover the trajectory of the robot. The initial and the final configuration are shown. An obstacle is reducing the size of the intermediate protective hull.

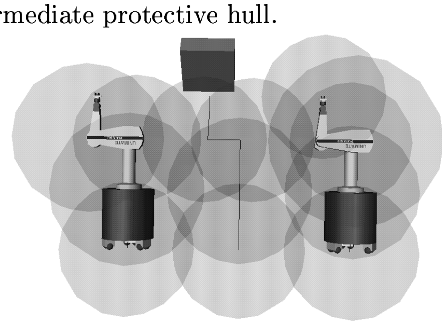

Figure 5: Protective hulls covering a trajectory

It is sufficient to describe a procedure that verifies the existence of a path between two consecutive protective hulls $\mathcal{P}_i^{\mathcal{R}}$ and $\mathcal{P}_{i+1}^{\mathcal{R}}$. By applying this procedure repeatedly the condition of feasibility (5) can be ensured.

We will make the assumption that every point on a rigid body b moves on a straight line as b transitions from q_i to q_{i+1}. This ignores the effect of rotation. However, this effect can be bounded and taken into account at a computational expense, when computing the protective hull of b. The justification for this assumption is that two adjacent configurations will be similar enough for this effect to be insignificant when the robot is close to an obstacle. This is a simplification but not an inherent limitation of the approach.

Using this assumption the path of each rigid body b can be examined independently. If a trajectory between q_i and q_{i+1} exists for all rigid bodies $b \in \mathcal{R}$, one exists for $\mathcal{R}$.

The existence of a trajectory $\mathcal{T}_{i,i+1}$ for a rigid body b from configuration q_i to q_{i+1} is guaranteed if the volume $V_{\mathcal{T}_{i,i+1}}^b$ swept by b along $\mathcal{T}_{i,i+1}$ is contained within the protective hulls of the configuration q_i and q_{i+1},

$$V_{\mathcal{T}_{i,i+1}}^b \subseteq \left(\mathcal{P}_i^b \cup \mathcal{P}_{i+1}^b\right). \qquad (6)$$

To verify condition (6) the union $\mathcal{U} = \mathcal{P}_i^b \cup \mathcal{P}_{i+1}^b$ is examined. If b can pass through $\mathcal{U}$ on a straight line trajectory form q_i to q_{i+1} then $V_{\mathcal{T}_{i,i+1}}^b$ is contained within $\mathcal{P}_i^b \cup \mathcal{P}_{i+1}^b$. Hence, condition (6) holds and $\mathcal{T}_{i,i+1}$ must be collision-free.

If for all rigid bodies $b \in \mathcal{R}$ the union of their protective hulls $\mathcal{P}_i^b \cup \mathcal{P}_{i+1}^b$ is large enough to allow a straight-line trajectory, we say that two consecutive protective hulls $\mathcal{P}_i^{\mathcal{R}}$ and $\mathcal{P}_{i+1}^{\mathcal{R}}$ are *connected*.

4.5 Forces Acting on the Strip

Whereas elastic material is homogeneous and its principal physical properties do not vary over its volume, this is not true for an elastic strip. In this framework an elastic strip can be seen as a two-dimensional grid of links and springs. Figure 6 illustrates that for the elastic strip $\mathcal{S} = (q_1, q_2, q_3)$ for an arm mounted on a mobile base.

The internal forces acting on the elastic strip are generated by the virtual springs attached to control points in subsequent configurations along the trajectory. Let $\mathbf{p}_j^i$ be the position vector of the origin of the frame attached to the j-th joint of the robot in configuration q_i. We use these points as control points. The internal contraction

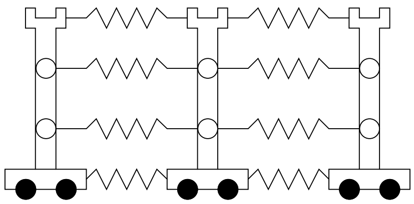

Figure 6: Principal structure of elastic strip

force $\mathbf{F}^{int}_{i,j}$ caused by the springs attached to joint j is defined as

$$\mathbf{F}^{int}_{i,j} = k_c \left(\frac{d_j^{i-1}}{d_j^i} (\mathbf{p}_j^{i+1} - \mathbf{p}_j^{i-1}) - (\mathbf{p}_j^i - \mathbf{p}_j^{i-1}) \right),$$

where d_j^i is the distance $\|\mathbf{p}_j^i - \mathbf{p}_j^{i+1}\|$ in the initial, unmodified trajectory and k_c is a constant determining the contraction gain of the elastic strip.

These forces cause the elastic strip to contract, maintaining a constant ratio of distances between every three consecutive configurations. Note that the force acting on the control points depends only on the local curvature of the elastic strip and not on its elongation.

The external forces are caused by a repulsive potential associated with the obstacles. For a point $\mathbf{p}$ this potential function is defined as

$$V_{ext}(\mathbf{p}) = \begin{cases} \frac{1}{2} k_r (d_0 - d(\mathbf{p}))^2 & \text{if } d(\mathbf{p}) < d_0 \\ 0 & \text{otherwise} \end{cases},$$

where $d(\mathbf{p})$ is the distance from $\mathbf{p}$ to the closest obstacle, d_0 defines the region of influence around obstacles, and k_r is the repulsion gain.

The external force $\mathbf{F}^{ext}_{\mathbf{p}}$ acting at point $\mathbf{p}$ is defined by the gradient of the potential function at that point:

$$\mathbf{F}^{ext}_{\mathbf{p}} = -\nabla V_{ext} = k_r (d_0 - d(\mathbf{p})) \frac{\mathbf{d}}{\|\mathbf{d}\|},$$

where $\mathbf{d}$ is the vector between $\mathbf{p}$ and the closest point on the obstacle.

4.6 Elastic Strip Modification

Let $\mathcal{S} = (q_1, q_2, q_3, \cdots, q_n)$ be an elastic strip. When $\mathcal{S}$ is subjected to the forces described in section 4.5, it is deformed by altering each of the configurations q_i in turn. To change a configuration according to the internal and external forces, these forces have to be mapped to joint torques. The choice of this mapping is task-dependent.

For collision avoidance in the absence of a task requirement, we use the Jacobian $J_{\mathbf{p}}$ associated with the point $\mathbf{p}$ at which the force $\mathbf{F}_{\mathbf{p}}$ is acting for this mapping. The joint torques $\mathbf{\Gamma}$ caused by $\mathbf{F}_{\mathbf{p}}$ are given by

$$\mathbf{\Gamma} = J_{\mathbf{p}}^T \mathbf{F}_{\mathbf{p}}. \qquad (7)$$

Joint limits can be avoided using a potential field function (Khatib 1986).

To implement collision avoidance during the execution of a task the joint torques computed in equation (7) have to be mapped into the null space associated with the Jacobian J of the task frame, as shown in equation (3).

The dynamic model of the system can be used to compute the joint displacements caused by the joint torques. The displacements for a configuration q_i define the new protective hull $\mathcal{P}'_i$, resulting in the modified elastic strip $\mathcal{S}' = (\mathcal{P}_1, \cdots, \mathcal{P}'_i, \cdots, \mathcal{P}_n)$. $\mathcal{S}'$ represents a valid trajectory, only if the protective hulls $\mathcal{P}_{i-1}$, $\mathcal{P}'_i$, and $\mathcal{P}_{i+1}$ are connected. This is verified using the procedure described in section 4.4.

If $\mathcal{P}'_i$ and $\mathcal{P}_{i+1}$ are not connected, the elastic strip $\mathcal{S}'$ becomes invalid. This means that the trajectory represented by $\mathcal{S}'$ cannot be proven to be collision-free, using the representation of local free space associated with $\mathcal{S}'$. In order to reconnect $\mathcal{P}'_i$ and $\mathcal{P}_{i+1}$ intermediate protective hulls are inserted into the elastic strip. By imposing constraints on the transition from $\mathcal{P}_i$ to $\mathcal{P}'_i$ this procedure can be guaranteed to succeed.

As obstacles recede from the vicinity of the elastic strip, the protective hulls of configurations increase in volume and potentially move closer together. This can result in protective hulls $\mathcal{P}_i$ and $\mathcal{P}_{i+2}$ to be connected. In that case $\mathcal{P}_{i+1}$ is redundant and can be removed.

5 Experimental Results

The results of a preliminary implementation are shown in Figure 7. The framework is applied to the Stanford Mobile Platform, a PUMA 560 robot arm mounted on a holonomic mobile base with a total of nine degrees of freedom. The elastic strip is represented by a set of intermediate configurations, displayed as lines connecting joint frames.

The approaching obstacle deforms the elastic strip to ensure obstacle avoidance. As the obstacle moves away, internal forces cause the elastic strip to assume the straight line trajectory. Our current implementation achieves an update rate

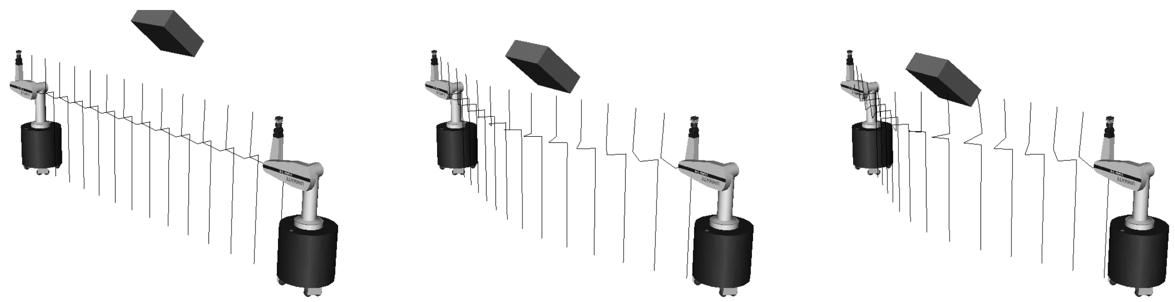

Figure 7: Elastic strip for a 9-dof robot incrementally modified by a moving obstacle

for the elastic strip in Figure 7 of 10 to 15 Hz on an SGI Indigo2. In the Figure the stationary obstacles of the environment have been removed.

6 Conclusion

The elastic strip framework is an efficient approach to real-time obstacle avoidance for robots with many degrees of freedom. It is particularly well suited for mobile manipulation, since it allows the integration of task-level behavior with collision avoidance in dynamic and uncertain environments.

An elastic strip represents the workspace volume swept by a robot along a pre-planned trajectory. This representation is incrementally modified by external, repulsive forces originating from obstacles to maintain a collision-free path. Internal forces act on the elastic strip to shorten and smoothen the trajectory.

To represent the volume swept by the robot the notion of a protective hull is introduced. A protective hull represents the local free space around a configuration and can be computed efficiently. A sequence of these hulls is used to contain the robot at any point along the trajectory, thus ensuring collision avoidance.

Experiments are presented demonstrating the elastic strip framework to operate in real-time for a trajectory of the Stanford Mobile Platform, a nine degree of freedom manipulator, in a dynamic environment.

7 Acknowledgments

The authors would like to thank Diego Ruspini and Kyong-Sok Chang for their helpful insights and discussion in preparing this paper. The financial support of Boeing, Nomadic Technologies, General Motors, and NSF (grant IRI-9320017) is gratefully acknowledged.

References

Arkin, R. C. (1987, August). Motor schema-based mobile robot navigation. *Int. J. of Robotics Research 8*(4), 92–112.

Carriker, W. F., P. K. Khosla, and B. H. Krogh (1989). An approach for coordinating mobility and manipulation. In *IEEE International Conference on Systems Engineering*, pp. 59–63.

Khatib, M., H. Jaouni, R. Chatila, and J.-P. Laumond (1997). How to implement dynamic paths. In *Proc. of the Int. Symposium on Experimental Robotics*, pp. 225–36. Preprints.

Khatib, O. (1986). Real-time obstacle avoidance for manipulators and mobile robots. *Int. J. of Robotics Research 5*(1), 90–8.

Khatib, O. (1987). A unified approach to motion and force control of robot manipulators: The operational space formulation. *IEEE J. of Robotics and Automation 3*(1), 43–53.

Khatib, O., K. Yokoi, K.-S. Chang, D. Ruspini, R. Holmberg, and A. Casal (1996). Vehicle/arm coordination and multiple mobile manipulator decentralized cooperation. In *Proc. of Int. Conf. on Intelligent Robots and Systems. IROS '96*, Volume 2, pp. 546–53.

Krogh, B. H. (1984). A generalized potential field approach to obstacle avoidance control. In *Robotics Research*, pp. MS84–484/1–15.

Latombe, J.-C. (1991). *Robot Motion Planning.* Boston: Kluwer Academic Publishers.

Nassal, U. (1996). Motion coordination and reactive control of autonomous multi-manipulator systems. *J. of Robotic Systems 13*(11), 737–54.

Quinlan, S. (1994). *Real-Time Modification of Collision-Free Paths.* Ph. D. thesis, Stanford University.

Quinlan, S. and O. Khatib (1993). Elastic bands: Connecting path planning and control. In *Proc. IEEE Int. Conf. on Robotics and Automation*, Volume 2, pp. 802–7.

Seraji, H. (1993). An on-line approach to coordinated mobility and manipulation. In *Proc. of Int. Conf. on Robotics and Automation*, Volume 1, pp. 28–35.

Yamamoto, Y. and X. Yun (1995). Coordinated obstacle avoidance of a mobile manipulator. In *Proc. of IEEE Int. Conf. on Robotics and Automation*, Volume 3, pp. 2255–60.